CMOS/BICMOS SELF-ASSEMBLING AND ELECTROTHERMAL MICROACTUATORS FOR TUNABLE CAPACITORS, GAP-CLOSING STRUCTURES AND LATCH MECHANISMS

Altug Oz* and Gary K. Fedder*†
*Department of Electrical and Computer Engineering and †The Robotics Institute
Carnegie Mellon University, Pittsburgh, PA 15213, USA

ABSTRACT

CMOS/BiCMOS MEMS micromovers that use the principles of self-assembly and electrothermal actuation have been designed, fabricated and tested. These micromovers exhibit lateral micro-positioning of up to 25 µm. Three main applications are demonstrated: tunable capacitors, gap-closing structures and latch mechanisms. A 2.17 to 1 capacitor tuning range was measured from 400 fF to 866 fF within a 5 V control voltage. Mechanical latch structures that operate by sequencing micromovers enable zero-power stand-by operation of the capacitors. Micromovers are also used to form 300 nm gaps, which are integrated into a microresonator design. Finite-element simulation of displacements of the lateral self-assembly and actuation match measured results to within 20%.

INTRODUCTION

There is an increasing interest for technologies to integrate MEMS actuators on CMOS or BiCMOS chips. The actuators should have small footprints and CMOS compatible control voltages (<5V). Electrothermal actuators can provide smaller footprints and smaller control voltages compared to the electrostatic actuators. They also provide large force and large displacements. However, thermal actuators consume more power than electrostatic actuators. Generally thermal actuators are also slower than the electrostatic actuators. Usually thermal time constants are longer than the electrical and mechanical time constants. To alleviate these two problems, the thermal mass of the actuators should be designed as small as possible.

Our prior electrothermal micromover design in a 20 µm by 200 µm area demonstrated 3.5 µm deflection with 18 mW heater power [1]. Lateral bending moments in the actuator are achieved by offsetting the metal layers embedded within the CMOS-MEMS beams. Larger displacement is desirable for many applications, but without increasing actuator footprint and power. Different techniques have been used to get larger displacements in compact areas. One of the techniques is to use both electrothermal and electrostatic actuation at the same time. One actuator design in a 0.03 mm^2 area produced 30 µm lateral deflection with 40 mW power [2]. Another design with the same technique was demonstrated for a RF MEMS switch [3]. A power of 400 mW was consumed during switching, but the 10 V electrostatic latch mechanism operated with close to zero continuous power. Another technique used current passed through V-shaped bent-beams anchored at two ends to cause a thermal expansion at the center of the actuator [4]. To increase the displacements, rotary actuators and inchworm designs were demonstrated by using multiple bent-beam actuators orthogonally [5]. For rotary actuator designs, the displacement was increased from 3 µm to 33µm, but power is increased from 40 mW to 375 mW.

LATERAL MICROMOVERS

CMOS-MEMS micromovers exploit lateral stress gradients by embedding metal layers that are offset from the centerline of the beam [1]. The folded-flexure microactuator in Fig.1 illustrates the change in metal offset along the length of the actuator beams. Built-in differences in residual stress in the aluminum and silicon dioxide layers create a gradient driving self-assembly upon micro-structural release. The released beam bends into an S-shape resembling the static mode-shape of a guided-end beam. Electrothermal actuation generates a stress gradient from the different temperature coefficients of expansion of the offset materials and, in most CMOS technologies, acts to retract the beam back to its layout position when heated. The length, width and metal offset of the actuator beams are the primary design parameters that determine displacement characteristics.
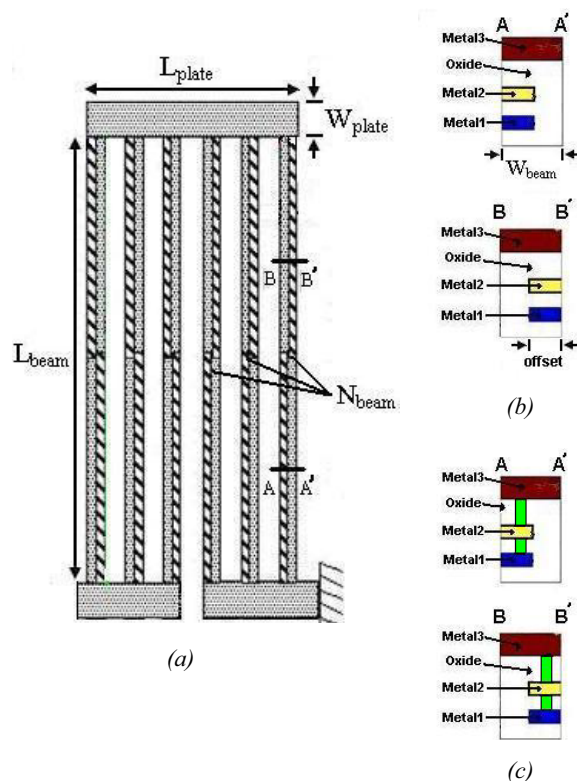

Figure 1. *(a) Layout and design parameters for a folded-flexure micromover, (b) Cross section of the micromover beams at two positions, showing the embedded metal offset, (c) Cross section of the micromover beams with vias between metal layers.*

Displacement magnitudes of the lateral self-assembly and actuation are verified quantitatively by finite element analysis (FEA), using Coventorware [6]. For FEA, a simulation

temperature, T_{set}, is calculated to model the lateral actuation magnitude upon release of the actuator.

$$T_{set} = -T_0 + T_{sim} + T_d \qquad (1)$$

where, T_{sim}, is the simulator initial temperature, which is 273 K, and T_d is the ambient temperature. T_o denotes the characteristic temperature, defined as the temperature at which a beam with embedded offset metal layers exhibits zero deflection relative to layout. To perform a simulation in Coventorware, the characteristic temperature for that type of actuator must be known. This information can be measured from lateral curl of a simple beam test structure, by determining the temperature at which the structure is completely straight. An SEM of a test cantilever structure at room temperature is shown in Fig.2(a). The verniers at the tip of the beam aid in measuring lateral displacement.

Micromovers were designed in the Jazz Semiconductor 4-metal 0.35 µm BiCMOS process by using the lower three metal layers. All of the test micromovers have a symmetric dual folded flexure design. An example simulation of displacement is shown in Fig.2(b) for device #1A, which has its design parameters given in Table 1. The characteristic temperature of 367 K used in the simulation was measured from a test beam with the same design parameters. The simulated self-assembly lateral displacement is 12.4 µm. The thermal coefficient of expansion (TCE) values, that are used in the simulations are 28.3 µ/K for metal layers and 0.4 µ/K for oxide layers.

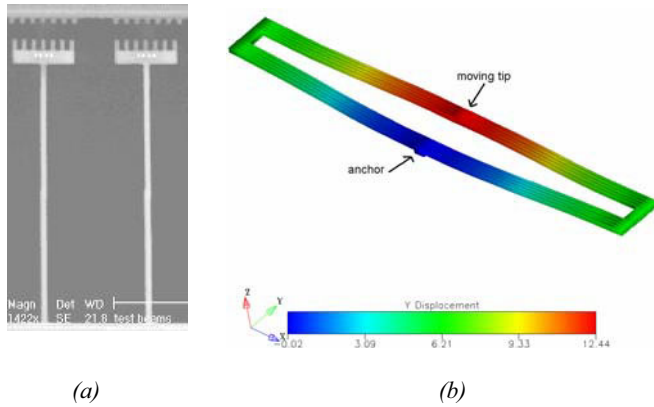*(a)*   *(b)*

Figure 2. *(a) Scanning electron micrograph (SEM) of test cantilever structures at room temperature, (b) Simulated self-assembly lateral displacement of device #1A.*
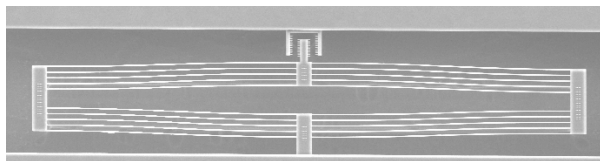

Figure 3. *SEM of a fabricated micromover in the Jazz process.*

Device #	L_{beam}	W_{beam1}	offset	L_{plate}	W_{plate}	N_{beam}	Via Between Metal layers
1A	200 µm	1.2 µm	0.6 µm	40 µm	10 µm	5	No
8A	200 µm	1.5 µm	0.9 µm	40 µm	10 µm	5	No
6B	200 µm	1.5 µm	0.9 µm	40 µm	10 µm	5	Yes
4B	100 µm	1.5 µm	0.9 µm	40 µm	10 µm	5	No

Table 1. *Design parameters for four dual folded-flexure micromover designs.*

Device #	Lateral self-assembly		Lateral electrothermal actuation		
	Measured displ.	Simulated displ.	T of the actuator	Measured displ.	Simulated displ.
1A	10.5 µm	12.4 µm	325 K	5.5 µm	4.3 µm
			350 K	10.5 µm	8.33 µm
			375 K	16 µm	12.27 µm
			400 K	21 µm	16.43 µm
			425 K	25.5 µm	20.46 µm
			450 K	---	24.48 µm
8A	1.8 µm	2.0 µm	325 K	4 µm	2.9 µm
			350 K	7.5 µm	5.5 µm
			375 K	10.5 µm	8.1 µm
			400 K	13 µm	10.5 µm
			425 K	15.5 µm	12 µm
			450 K	---	15.4 µm
6B	11 µm	12.8 µm			
4B	0.3 µm	0.4 µm			

Table 2. *Simulated and measured lateral displacement from self-assembly and electrothermal actuation.*

An SEM of the fabricated device #1A is shown in Fig.3. Measured and simulated displacement magnitudes of the lateral self-assembly and electrothermal actuation for different micromover test structures are given in Table-2. The temperatures in Table-2 are set with external heat sources and thermal sensing equipment for monitoring the temperature. Measured and simulated results match within 20%.

Some new techniques are used to improve the maximum displacement from the same actuator area. One technique is using vias between metal layers, as shown in Fig.1(c), to increase the lateral motion at the tip of the actuator. Device #6B has same design parameters as device #8A with the addition of the vias between metal layers. Device #6B has 6.1 times larger lateral displacement compared to device #8A for self-assembly.

Mechanical frequency response due to electrothermal actuation was measuried optically using a MIT microvision system [7]. Measurement results are shown in Fig.4 for a micromover in the Jazz process with the design parameters: L_{beam}= 168 µm, W_{beam1}= 1.5 µm, W_{beam2}= 0.9µm, L_{plate}= 43 µm, W_{plate} = 12 µm, and N_{beam}= 5. The 3dB bandwidth is 178 Hz. The measured mechanical resonant frequency (f_{res}) in Fig.4 is 26.3 kHz. Thermal bandwidth of the actuator is smaller than the mechanical bandwidth, so the system is dominated by the first-order thermal
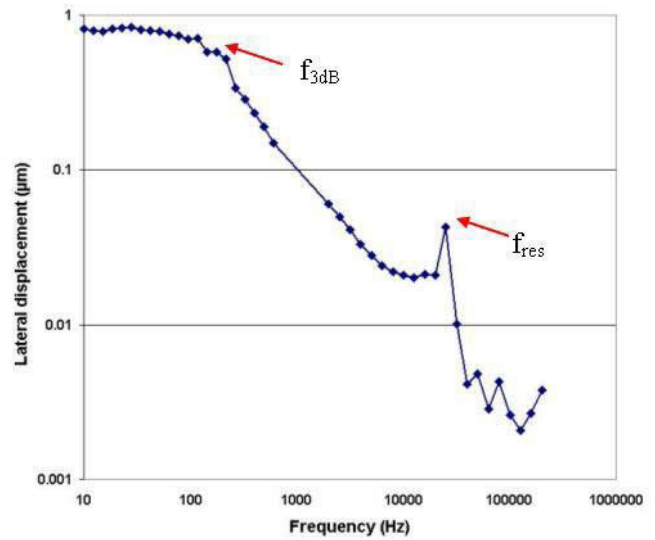

Figure 4. *Mechanical frequency response of a dual folded-flexure micromover during electrothermal actuation.*

response at frequencies below the mechanical resonance. The calculated 3dB bandwidth value from an equivalent first-order thermal model is 127Hz. The estimated thermal conductance and capacitance in the model are 5.832×10^{-5} W/K and 6.51×10^{-8} J/K, respectively.

LATERAL LATCH MECHANISM

Electrothermal actuators consume far more power in continuous operation compared to electrostatic actuators. It is advantageous to latch the micromovers into desired positions to eliminate continuous power supply. One basic latch mechanism is a "peg" in a slot, shown in Fig.5. The two micromovers start at zero power with the peg and one of the slots in an engaged position. This engaged position is formed through self-assembly of the micromovers. In the first actuation step, the latch micromover is actuated, pulling the slot away from the peg. After this, the device micromover is actuated to a new position corresponding to a different second slot. In the second step, heating power to the latch micromover is turned off and the peg becomes engaged with the second slot. In the third step, heating power to the device micromover is turned off, and the slot and peg contact each other keeping the device in its new position.

LATCHED TUNABLE CAPACITOR

Several tunable RF capacitors with a latching mechanism were fabricated in the Jazz process. A representative comb-finger capacitor design is shown in Fig.6. The latching function demonstrated upon release is shown in Fig.7(a) and corresponds to $C_{MIN} = 280$ fF. The second in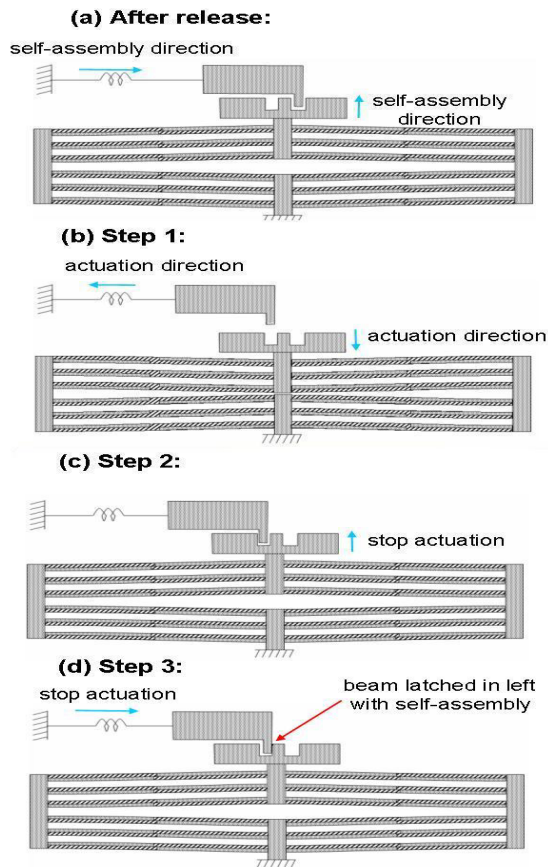tended C_{MAX} latch state was not functional because the comb fingers could not engage. The alternate second latched position is shown in Fig.7(b) and corresponds to $C_{MAX} = 380$ fF, when the comb truss beams contact mechanically.

The measured tuning range of 36% is believed to be limited by a thin layer of sidewall polymer that acts as a dielectric spacer. This polymer is deposited during the CMOS-MEMS dielectric etch.. The comb engagement problem was due to bloat of the metal-4 layer, from which the mask defining the finger sidewalls was formed, and exacerbated by further comb finger widening from polymer deposited on the sidewalls.

Alternate capacitor designs were made with long interdigitated beams operating in a parallel-plate mode. This design has a measured minimum capacitance of 400 fF when the beams are centered with maximum gap and a maximum capacitance of 866 fF when the beams are actuated and touching, similar to the latch state in Fig.7(b) (but without the comb fingers). These limiting capacitance values, corresponding to a 2.17:1 tuning range, are about twice as large as the previous generation design [1]. The simulated values of $C_{MIN} = 310$ fF and $C_{MAX} = 800$ fF match with the measured values within 25%. The latch mechanism also functions for this design.

These sidewall parallel-plate capacitors are used in a voltage controlled oscillator (VCO) that provides 700 MHz frequency tuning range around a 2.45 GHz center frequency [8]. Similar capacitors are used in a RF filter to provide 490 MHz frequency tuning range around 2.1 GHz center frequency [8]. This capacitor design also enabled a low-power VCO design, by having a high quality factor over 30 for 1.5 GHz to 2.5 GHz [9].

GAP CLOSING STRUCTURE

Another application of the micromovers is in assembling nanometer-scale sidewall gaps for large capacitance and large
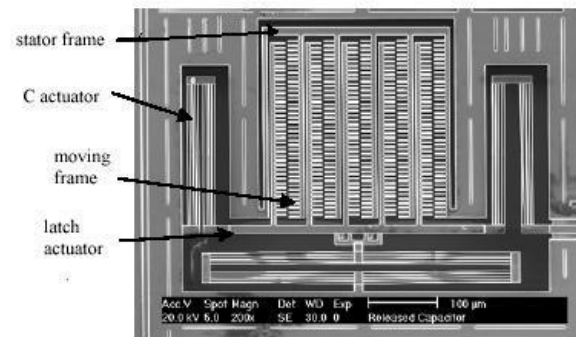

Figure 6. *An unengaged comb-finger tunable capacitor.*
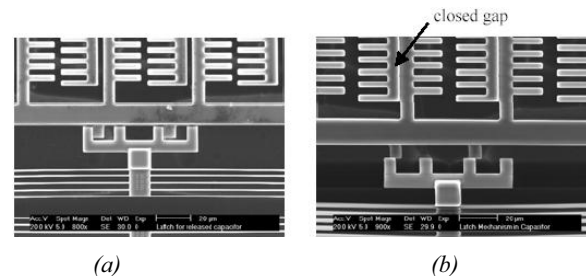

(a)   *(b)*

Figure 7. *Capacitor latching. (a) A disengaged comb finger latch state, (b) A different latch state, where the comb truss beams contact mechanically.*

Figure 5. *Sequential steps for lateral latch mechanism.*

electrostatic force per area. Desirable gap sizes range from about 50 to 500 nm. Such small gaps are particularly useful for improving the gain of high-frequency microresonators. Conventional optical lithography and etching limits gap width in the CMOS microstructures to around 0.5 µm. Smaller gaps have been made in other micromachining processes, for example by forming a thin sacrificial oxide layer between silicon or polysilicon electrodes. In our assembly approach, the gap as drawn in layout is much larger than the final dimension, as depicted in Fig.8. One electrode of the gap is a resonator, exemplified by the fixed-fixed beam in Fig.8. A micromover shifts the other electrode in the direction to narrow the gap. A self-assembly micromover is ideal for this application, requiring zero power. A rigid limit stop sets the desired final gap value. Since the limit stop edge and the beam edge face the same direction, any global manufacturing variation in the sidewall etch will not affect the gap dimension. Theoretically, the gap can be set to an arbitrarily small value, however the practical minimum gap will be determined by the surface roughness of the sidewalls.

The gap closing mechanism is fabricated in the Jazz process for a cantilever resonator application. The gap closing result is given in Fig.9. The initial gap between the resonator and the micromover electrode was 1.1 µm, while the gap between the micromover and the limit stop was 0.8 µm. A 0.3 µm nanometer-scale gap was achieved after the release etch. For reference, the width of the beams on the resonator are 1.4 µm.
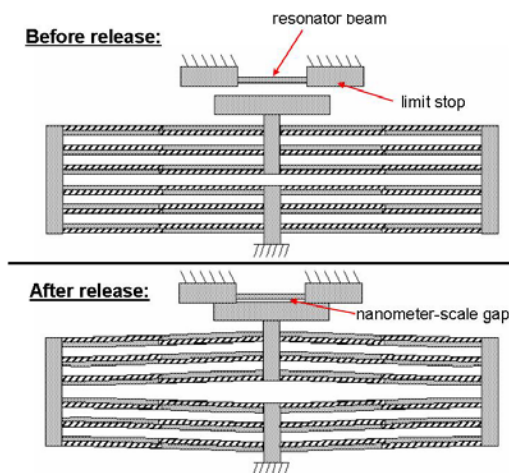

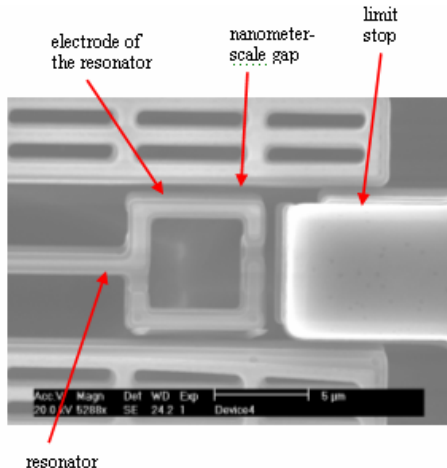**Figure 8.** *Gap closing mechanism by using micromover self-assembly.*

Figure 9. *SEM of a nanometer scale gap-closing mechanism.*

CONCLUSIONS

Maximum displacements of 10.5 µm for self-assembly and 25.5 µm for actuation enable applications where relatively large stroke in a compact footprint are needed. The micromovers are capable of sufficient motion to engage relatively long comb fingers. A 8:1 C_{MAX}:C_{MIN} tuning ratio is expected by compensating the metal-4 bloat in future layout. Design optimization may increase the tuning ratio further. The reasonable match between measured and simulated micromover displacement values verifies that the simulations are adequate for predictive design, but that second-order model refinement remains to be done. Zero-power standby capacitor tuning was demonstrated using the latch mechanism. Future work will investigate refinement of actuated latch mechanisms and quantify the improvement in resonator performance by using gap-closing mechanisms.

ACKNOWLEDGEMENT

REFERENCES

1. A. Oz, G. K. Fedder, "RF CMOS-MEMS capacitor having large tuning range," in *Proc. 2003 IEEE Int. Conference on Solid-State Sensors and Actuators (Transducers' 03),* Boston, MA, June 2003, Page(s): 851-854.

2. X.-Q. Sun, X. Gu, and W. N. Carr, "Lateral in-plane displacement microactuators with combined thermal and electrostatic drive," in *Proc. Solid-State Sensor and Actuator Workshop*, Hilton Head, SC, June 1996, pp. 152–155.

3. Ph. Robert, D. Saias, C. Billard, S. Boret, N. Sillon, C. Maeder-Pachurka, P. L. Charvet, G. Bouche, P. Ancey, P. Berruyer, "Integrated rf- mems switch based on a combination of thermal and electrostatic actuation," in *2003 IEEE Int. Conference on Solid-State Sensors and Actuators (Transducers' 03)*, Boston, MA, June 2003. Page(s): 1714-1717.

4. L. Que, J.-S. Park, and Y. B. Gianchandani, "Bent-beam electrothermal actuators -I: single beam and cascaded devices," in *J. MEMS*, vol. 10, pp. 247–254, June 2001.

5. J.-S. Park, L. L. Chu, A. D. Oliver, and Y. B. Gianchandani, "Bent-beam electrothermal actuators—Part II: Linear and rotary microengines," in *J. MEMS*, vol. 10, pp. 255–262, June 2001.

6. Coventor web page, http://www.coventor.com.

7. D. Freeman, A. Aranyosi, M. Gordon, S. Hong, "Multi-dimensional Motion Analysis of MEMS Using Computer Microvision", *Solid State Sensor & Actuators Workshop*, Hilton Head Is., SC, 1998, p. 150-155.

8. D. Ramachandran, A. Oz, V. K. Saraf, G. K. Fedder, T. Mukherjee, "MEMS-enabled reconfigurable VCO and filter", *2004 IEEE MTT-S Int. RFIC Symposium Dig.,* June 2004.

9. V. K. Saraf , D. Ramachandran, A. Oz, G. K. Fedder, T. Mukherjee, "Low-Power LC-VCO using integrated MEMS passives", *2004 IEEE MTT-S Int. RFIC Symposium.Dig.,* June 2004.